Communications Research Centre

THE ATTITUDE DYNAMICS OF HERMES AFTER TERMINATION OF THREE-AXIS STABILIZATION

by

F.R. VIGNERON AND W.E. KRAG

CRC REPORT NO. 1354

Department of Communications
Ministère des Communications

OTTAWA, FEBRUARY 1982

COMMUNICATIONS RESEARCH CENTRE

DEPARTMENT OF COMMUNICATIONS
CANADA

THE ATTITUDE DYNAMICS OF HERMES AFTER TERMINATION OF THREE-AXIS STABILIZATION

by

F.R. Vigneron* and W.E. Krag**

(Space Technology and Applications Branch)

* Department of Communications, Ottawa, Canada

** Massachusetts Institute of Technology Lincoln Laboratory, Lexington, Mass.

CRC REPORT NO. 1354

February 1982

OTTAWA

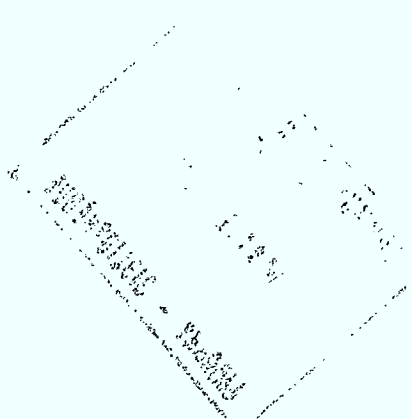

TABLE OF CONTENTS

ABSTRACT 1

1. INTRODUCTION 2

2. DESCRIPTION OF HERMES, ETS, AND THE OPTICAL OBSERVATIONS 3

3. THEORETICAL PRINCIPLES AND ANALYTICALLY-DERIVED RESULTS 3

3.1 Initial States, Day 329, 1979 5

3.2 Overview of the Dynamics of the Transition to Flat Spin 5

3.3 Analysis of ω_2 and β for Short Time Intervals 6

3.4 The Rate $\dot{\psi}$. 10

3.5 Computer-Generated Display of Motion 10

3.6 Theory of Long Term Behaviour of the Flat Spin Rate 11

4. CORRELATION OF OBSERVATIONS AND ANALYTICALLY-DERIVED RESULTS 11

4.1 Detailed Correlation for the Transition to Flat Spin 12

4.2 Flat Spin and Despin 13

4.3 The Double Peak and Array Deformation 14

5. CONCLUSIONS 14

6. REFERENCES 15

THE ATTITUDE DYNAMICS OF HERMES AFTER TERMINATION OF THREE-AXIS STABILIZATION

by

F.R. Vigneron and W.E. Krag

ABSTRACT

In late 1979, Hermes, an experimental geostationary communications satellite, experienced an earth sensor malfunction which resulted in its loss of control and subsequent transition from 3-axis stabilization to spin about its maximum-moment-of-inertia axis. During and after the transition, the sun's reflections from the satellite were detected and monitored at the experimental test site (ETS) for the Ground Based Electro Optical Deep Space Surveillance System (GEODSS) in New Mexico. In this report, the satellite's attitude dynamics are deduced by correlating the GEODSS ETS observations with dynamics analysis and simulation. The transition to spin took about 15 days. Thereafter, the rate of spin decayed to zero in about 70 days due to solar pressure. The GEODSS ETS observations also provide data on the relative misalignment and bending of the two solar sails of the satellite.

The material in this report was presented at the 12th Norad Spacecraft Identification Conference 13-15th August 1980.

A part of the work reported in this document was performed at Lincoln Laboratory, with the support of the Department of the Air Force. The views and conclusions contained in this document should not be interpreted as necessarily representing the official policies, either expressed or implied, of the United States Government.

1. INTRODUCTION

On Day 329 of 1979, the Hermes satellite experienced an earth sensor malfunction which, in conjunction with degraded telemetry and battery performance and anomalous thruster firing, resulted in a shutdown of the satellite. The experimental communications program was thus terminated after operating for almost twice the planned mission duration.

The satellite configuration showing major control components and solar sails is given in Figure 1. The satellite was launched into orbit with a Thor Delta 2914 in January 1976. It was spin-stabilized with its solar array stowed during transfer orbit, apogee motor burn, and until it was located on station at 116° West longitude. In the subsequent attitude acquisition sequence the satellite was despun, the solar array was deployed, a momentum wheel was spun up, and an on-board 3-axis stabilization system was activated for normal operation in geostationary orbit.

The type of control system used for Hermes relies on gyroscopic stiffness contributed by the momentum wheel for roll and yaw stability. An on-board controller activates thrusters to trim out the small attitude errors sensed by the earth sensor. Each of the solar sails has an independent sun sensor and tracking mechanism, and normally faces the sun. When operating normally, the basis for stability is essentially the well known dual-spin principle with a minimum moment of inertia configuration, the central body being the 'platform' and the momentum wheel being the 'rotor'. If the wheel despins, a loss of dual-spin stability results and the motion tends to a spin about the maximum moment of inertia (yaw) axis.

Following the earth sensor malfunction on Day 329, 1979, the on-board controller transferred automatically to a failure-protect mode in which the wheel speed was constant. Shortly thereafter, a roll-yaw nutation cone and pitch rotation were induced by the thrusters. Within about 15 minutes, the solar array was unable to track the sun, resulting in a drain (without solar recharge) on the batteries. The batteries were designed to provide limited power during eclipse and also were somewhat degraded after nearly four years of operation. Consequently, they were able to provide spacecraft and momentum wheel operation for a few hours at most. Thereafter, the wheel lost its drive power, the wheel momentum transferred to the spacecraft body, and a substantial increase of the spin about the pitch axis resulted. Thus, within several hours of malfunction, the satellite state became dynamically unstable, with a spin about pitch (the minimum moment of inertia axis) and a roll-yaw nutation. Without battery power, the satellite lost its capability to transmit RF signals and to receive commands.

From Day 331 of 1979 to mid 1980, MIT Lincoln Laboratory periodically recorded the sun's reflections from Hermes with an optical telescope of the Ground Based Electro Optical Deep Space Surveillance (GEODSS) Experimental Test Site near Socorro, New Mexico. During this time, Hermes made the transition from the state of unstable spin about pitch to stable flat spin about the yaw axis; subsequently, the rate of flat spin changed substantially. The GEODSS ETS has two 31-inch aperture tracking telescopes, each mounted on a Boller and Chevins equatorial mount. The observations are made with special low-light television cameras mounted at the focal plane of earth telescope, and are displayed in real time on television monitors in a control building adjacent to the telescopes.

In this paper, the GEODSS ETS observations of Hermes are first described. Since a knowledge of theoretical dynamics is necessary to interpret the observations, the relevant principles and related information are presented next. Then the observations and dynamics theory are correlated. Finally, conclusions relevant to satellite dynamics, satellite operations, and optical analysis are given.

2. DESCRIPTION OF HERMES, ETS, AND THE OPTICAL OBSERVATIONS

The Hermes satellite and mission are described in Reference 1 and associated references. The physical geometry of Hermes is shown in Figures 1 and 2. The satellite is about 15 metres long tip-to-tip and is about 1.5 m. wide. The front of the array is largely covered with solar cells which, with the cell covers and optical filtering, appear to be blue in colour. The front and back decks are covered with kapton. The top and bottom panels of the satellite body and the heat pipe radiator are polished aluminium. When the satellite is operating normally, the central body tracks the earth, and each of the two solar sails track the sun independently by rotating slowly about the long axis relative to the central body. The arrays are tensioned with a silver-plated 1-3/8" diameter BISTEM boom extending from the central body behind the kapton sheet, as seen in Figure 2.

The GEODSS ETS uses 31-inch aperture tracking telescopes mounted on Boller and Chevins equatorial mounts. Signals from special low-light television cameras mounted at the focal plane of each telescope are displayed on television monitors at an operator console in a control building located about 200 feet from the telescopes. The telescopes are computer-driven by selected operator commands to a minicomputer. Hermes was tracked and displayed in a mode where the satellite remains stationary on the television monitor and the star background moves horizontally across the screen. The satellite brightness is measured directly by the video signal from an intensified Ebsicon video camera mounted on the telescope. The video signal over a selected area containing the satellite (point) image is integrated and recorded on a strip chart at the standard TV rate of 30 samples per second. The satellite brightness is measured by comparison with the signal from calibration stars in the vicinity. The GEODSS ETS is located in New Mexico at about 34° north latitude and 107° west longitude. Capabilities of the facility are described more fully in Reference 2.

Figures 3 and 4 typify the strip chart output of the intensity variations of the reflections which were observed from Day 331, 1979 until Day 60, 1980. A summary of the data is given in the Observations column of Table 1. Familiarity with information provided by dynamics theory is essential for interpretation of the data.

3. THEORETICAL PRINCIPLES AND ANALYTICALLY-DERIVED RESULTS

This section summarizes the knowledge of the initial dynamic state of Hermes immediately following the malfunction of Day 329, 1979, and then presents the theory of the ensuing motion.

TABLE 1
Sightings of Hermes by GEODSS

Day No.	Days after Sensor Malfunction	Observation	Interpretation
331/79	2	Major light flashes. Not recorded.	The satellite has lost earth lock.
333/79	4	Major light flashes. Not recorded.	
335/79	6	Major flashes. The brightness variations show a period of 24 seconds and a series of bright flashes which, in retrospect, indicate a period of about 900 seconds.	The satellite dynamic motion has a nutation cone of about 30^{o} and a spin period of about 48 seconds. The nutation period is 300 seconds.
336/79	7	Major flashes. The short period is 30-32 seconds and there are long flashes indicating a longer period.	The nutation cone is in the process of increasing from 30^{o} to 75^{o}.
337/79	8	Major flashes. The short period is 40 seconds and there are long flashes indicating a longer period.	
338/79	9	The data are not definitive. The periods are 100 to 150 seconds, and about 900 seconds.	
339/79	10	The short period is no longer clearly present. The 900 second period remains, and, in retrospect, the variations show signs of being three 300 second periods. The motion is not stable. Some of the recorded flashes have a double peak.	The satellite is close to flat spin, with a cone angle of $80\text{-}85^{o}$.
341/79	12	The long second period is clearly evident, by the double peak, and its value is 285 ± 3 seconds.	
345/79	16	Sightings in the early evening did not detect the satellite (19:00 local time). At about 22:00 the satellite became visible.	The satellite is in stable flat spin about its yaw axis. The double-peaked pattern is reflected from the two BISTEMs of the solar array; the data implies a mean dihedral-related angle of 3.5 degrees. The varying peaks are probable reflections from the front of the satellite or its solar array.
346/79	17	The pattern is very regular, with one period of 292 seconds. One set of brightness signals is about 11th magnitude, consists of two sharp peaks of 3 second width each, about 3 seconds apart. A second set of signals consists of broad 30 second peaks varying with time from more than 10th magnitude to less than 13th magnitude.	
347/79	18	Sighting attempted early evening with no success.	
350/79	21	Very similar to Day 346, with a period of 309 seconds.	
17/80	42	As per Day 346, with a period of 540 seconds.	The satellite is despinning, and the probable cause is solar-pressure induced propellor torque.
18/80	43	As per Day 346, with a period of 557 seconds.	
23/80	48	As per Day 346, with a period of 673 seconds.	
26/80	51	As per Day 346, with a period of 774 seconds.	
29/80	54	As per Day 346, with a period of 1646 seconds.	
52/80	77	As per Day 346, with a period of 2808 seconds.	

3.1 INITIAL STATES, DAY 329, 1979

Prior to the earth sensor malfunction on Day 329, the satellite was three-axis stabilized in the configuration depicted in Figure 1. As noted in the Introduction a nutation cone was induced by the thrusters immediately following the earth sensor malfunction. Within about 15 minutes, the solar array lost sun lock and several hours later, the momentum wheel lost its drive power, and despun within about 30 minutes. With despin, the wheel momentum transferred to the satellite body, causing a substantial spin about pitch.

The satellite parameters are listed in Table 2. The states summarized above are tabulated in Table 3.

TABLE 2

Hermes Parameters, November 1979

Moment of Inertia, A (Slug-ft^2)	$832.6 + 3.3 \sin^2\gamma$
Moment of Inertia, B (Slug-ft^2)	71.5
Moment of Inertia, C (Slug-ft^2)	$858.8 - 3.3 \sin^2\gamma$
Wheel Speed (rpm)	4290
Wheel Inertia (Slug-ft^2)	0.0376
H (lb-ft-sec)	16.8
Array Angle, γ (Deg)	about 239

3.2 OVERVIEW OF THE DYNAMICS OF THE TRANSITION TO FLAT SPIN

The state immediately after wheel despin is unstable dynamically, and will change with time to a state of flat spin. The theory of the transition is complex conceptually and mathematically, but is available in the literature in detail for some types of satellites (for example, Refs. 3-4). For the Hermes configuration detailed modelling and results are not available. The general principles are explained herein, using angular momentum and energy concepts.

The satellite and its coordinates are shown schematically in Figure 5. The satellite is slightly non-rigid and is rotating while deforming about its mass center in an environment free of external forces and torques. Its angular momentum vector, $\underline{H}$, is constant and fixed in direction in inertial

TABLE 3

Dynamic States of Hermes

	Before Sensor Malfunction	Immediately Before Despin	Immediately After Despin	Pure Spin About Pitch	Pure Spin About Yaw
Wheel Speed (rpm)	4285	4270	0	0	0
ω_2 (rad/sec)	7.3×10^{-5}	3.1×10^{-3}	0.238	0.253	0
H (ft-lb-sec)	16.8	18.1	18.1	18.1	18.1
β (deg)	0	20	20	0	90
γ, north (deg)	239	239*	239*	239*	239*
γ, south (deg)	239	239*	239*	239*	239*
T (lb-ft)	–	–	2.05	2.2910	0.1913
P_ω (sec)	86,400	2028	26.4	24.8	0
P_ψ (sec)	–	–	297.3	297.3	297.3

* *Values are uncertain*

space due to an absence of significant external forces and torques. The reference frame $\{0XYZ\}$ is inertial and is aligned so that 0Y is parallel to $\underline{H}$. The $\{01, 02, 03\}$ are mean axes, assigned to the satellite in such a way that the mean momentum of vibratory deformation about them is zero. They are also principal axes if the deformation is zero. The moments of inertia about the spacecraft axes are denoted by A, B, C. In the following, C>A>B as per Table 2. The magnitude of $\underline{H}$ is denoted by H.

A particular attitude motion state consists of a unique combination of nutation and spin. Each state can be categorized by a value of the kinetic energy, T, for a particular H, A, B, and C. If T and H are constant, the corresponding physical motion is periodic. The kinetic energy of attitude dynamics of an arbitrary state is approximately

$$T = \frac{1}{2} (A\omega_1^2 + B\omega_2^2 + C\omega_3^2) \qquad (1)$$

The principle of conservation of momentum dictates that

$$H^2 = A^2\omega_1^2 + B^2\omega_2^2 + C^2\omega_3^2 \tag{2}$$

Figure 6 depicts the relationship between H and its components. ω_1, ω_2. and ω_3 are the angular rates of $\{0\ 1\ 2\ 3\}$ relative to $\{OXYZ\}$.

For a state of motion where the spacecraft is in pure spin about the 02 (minimum moment of inertia) axis, velocities and kinetic energy are constant with values

$$\omega_{1i} = \omega_{3i} = 0; \quad \omega_{2i} = H/B \tag{3a}$$

$$T_i = \frac{1}{2} B\omega_{2i}^2 = \frac{1}{2}\frac{H^2}{B} \tag{3b}$$

For a state of motion where the spacecraft is in pure spin about its maximum moment of inertia axis, the 03 axis, the angular velocities and kinetic energy are constant with values

$$\omega_{1f} = \omega_{2f} = 0 \ ; \ \omega_{3f} = H/C \tag{4a}$$

$$T_f = \frac{1}{2} C\omega_{3f}^2 = \frac{1}{2}\frac{H^2}{C} \tag{4b}$$

The subscripts 'i' and 'f' denote 'initial' and 'final', respectively. Equations (3b) and (4b) represent the states of maximum and minimum possible energy, respectively (note that H is constant and C is greater than B) and are the extremities of the possible states. Between these extremities, the motion states which consist of combination of spin and nutation are periodic with one or more distinguishable periods. The motion described by Equations (4) is the 'flat spin' or maximum moment of inertia spin case; it is the only stable motion in the long term. All other motions [including the state corresponding to Equation (3)] tend to this lowest energy state with time, as the kinetic energy of motion is dissipated due to fuel slosh, structural frictions, and the nutation damper.

The Euler equations which provide details of nutation and spin exactly when solved, are

$$\frac{d}{dt}(A\omega_1) - (B-C)\omega_2\omega_3 + f_1 = 0 \tag{5a}$$

$$\frac{d}{dt}(B\omega_2) - (C-A)\omega_3\omega_1 + f_2 = 0 \tag{5b}$$

$$\frac{d}{dt}(C\omega_3) - (A-B)\omega_1\omega_2 + f_3 = 0 \tag{5c}$$

where f_1, f_2, and f_3 denote internal torques due to structural damping and a nutation damper and corresponding non-zero cross products of inertia.

If the natural damping forces are small (which is the situation for Hermes and most satellites), an approximation of the motion can be obtained by solving Equation (5) with $f_1 = f_2 = f_3 = 0$ and A, B, and C assumed to be the constant rigid satellite values. Such a solution shows the characteristic nutation behaviour and spin periods, and will be described in more detail later.

The rate of change of T is given by

$$\frac{d}{dt} T = - (\omega_1 f_1 + \omega_2 f_2 + \omega_3 f_3) \tag{6}$$

Equation (6) is obtained by multiplying Equations (5a), (5b), and (5c) by ω_1,ω_2, ω_3, and adding and rearranging. From Equation (6) it is seen that if the f's are small, then T can be regarded as essentially constant. This approximation is valid for time intervals of the order of a few nutations and spin periods. For Hermes, T can be regarded as constant for time period of 2-3 hours. However, over the long term T decays to the minimum value given by Equation (4b).

A summary of the parameter values for the Hermes states at various stages after the earth sensor malfunction are given in Table 3. The initial states were not directly obtainable from telemetry and to some extent are derived from a knowledge of the spacecraft's behaviour under conditions similar to those present on Day 329.

For time intervals of the order of a few hours for Hermes, the motion state is constant. Two particular periodic motions will be examined for later correlation with GEODSS observations, namely, that associated with ω_2 and that associated with the nutation rate, $\dot{\psi}$.

3.3 ANALYSIS OF ω_2 AND β FOR SHORT TIME INTERVALS

The variable ω_2 defines the state of spin about the pitch axis. As will be discussed later, reflections of the sun from flat surfaces such as the solar sail would be expected to correlate with ω_2. Equations (1-2) can be rearranged to yield:

$$\omega_1^2 = \frac{1}{A(C-A)} \left\{ B(B-C)\omega_2^2 - H^2 + 2TC \right\} \tag{7a}$$

$$\omega_3^2 = \frac{1}{C(C-A)} \left\{ B(A-B)\omega_2^2 + H^2 - 2AT \right\} \tag{7b}$$

Substitute Equations (7) into Equation (5b), and assume f_2 equal to zero and B a constant, to obtain

$$\dot{\omega}_2 = \pm \left[\frac{\left\{B(A-B)\omega_2^2 + (H^2-2AT)\right\}\left\{B(B-C)\omega_2^2 - (H^2-2CT)\right\}}{CB^2A} \right]^{1/2} \tag{8}$$

Equation (8) can be presented in the factored form

$$\dot{\omega}_2 = \pm \left[\frac{(A-B)(B-C)}{CA} (\omega_2 - W_1)(\omega_2 - W_2)(\omega_2 - W_3)(\omega_2 - W_4) \right]^{1/2} \tag{9}$$

where

$$W_1 = \frac{H}{B} \left[\frac{B}{C-B} \left(2C \frac{T}{H^2} - 1\right) \right]^{1/2} ; \quad W_4 = - W_1, \tag{10a}$$

$$W_2 = \frac{H}{B} \left[\frac{B}{A-B} \left(2A \frac{T}{H^2} - 1\right) \right]^{1/2} ; \quad W_3 = - W_2. \tag{10b}$$

From Figure 6 the direction cosine, m, between the constant vector $\underline{H}$ and the OZ axis is related to ω_2 by

$$m \triangleq \cos\beta = \frac{B\omega_2}{H} \tag{11}$$

By combining Equations (11), (9) and (10), the following first-order differential equation is obtained:

$$\dot{m} = \pm \frac{H}{B} \left[\frac{(A-B)(B-C)}{AC} (m - m_1)(m - m_2)(m - m_3)(m - m_4) \right]^{1/2} \tag{12a}$$

where

$$m_1 = \frac{B}{C-B} \left[\frac{2CT}{H^2} - 1 \right]^{1/2}, \quad m_4 = - m_1 , \tag{12b}$$

$$m_2 = \frac{B}{A-B} \left[\frac{2AT}{H^2} - 1 \right]^{1/2}, \quad m_3 = - m_2 .$$

The roots of Equations (12) are plotted vs T in Figure 7, for the Hermes parameters of Table 2. The sets of phase planes of Figures 8 and 9, which are derived from Equations (9) and (12), demonstrate the following:

(a) β increases from 0° to 90° as T decreases from $H^2/2B$ to $H^2/2C$, as stated earlier (Figure 9).

(b) When T is between $H^2/2B$ and $H^2/2A$, $\omega_2(t)$ is a spin motion (Figure 8). The corresponding range for m is 1 and $[B(C-A)/A(C-B)]^{\frac{1}{2}}$, or $\beta = 0°$ and $\beta = 87.2°$ (Figure 9).

(c) When T is between $H^2/2A$ and $H^2/2C$, $\omega_2(t)$ is oscillatory (Figure 8). The corresponding angular range is 87.2° to 90°. Physically the characteristic motion is a flat spin about yaw of rate H/C with a superimposed rocking motion about the 02 axis. The rocking disappears as T tends to $H^2/2C$.

(d) When β is less than about 82°, the roots W_1 and W_2 are virtually equal (Figure 7). For this range of β, the satellite can be regarded as symmetric with C = A. The phase planes such as Figure 8 show that the spin rate, ω_2, can be regarded as essentially constant and equal to W_1 or W_2, and thus depends on T as per Equations (10). 99% of the dissipative energy is associated with this range. The relationship of ω_2 to β and the period P_ω, are (see Equation 11):

$$\omega_2 = \frac{H}{B} \cos\beta \tag{13a}$$

$$P_\omega = 2\pi/\omega_2 : \tag{13b}$$

3.4 THE RATE $\dot{\psi}$

$\dot{\psi}$ is related to the nutation rate of the satellite. As will be discussed later, reflections of the sun from surfaces such as the north or south panels or support booms of the sails correlate with $\dot{\psi}$.

The satellite can be regarded as symmetric with A = C when β is less than about 82° and this assumption is adequate for discussion of GEODSS observations of nutation. The solution of Equations (5) with A = C and the f's equal to zero is available in standard texts (References 3 or 4). The expression for $\dot{\psi}$ can be written as H/C, and hence the associated period is

$$P_\psi = 2\pi C/H. \tag{14}$$

Note that P_ψ is constant and does not depend on T or β, and also equals the flat-spin period [Equation 4(a)].

3.5 COMPUTER-GENERATED DISPLAY OF MOTION

To provide a physical understanding of the motion, a qualitative computer-graphics animated display was developed at the Communications Research Centre. The animation system consists of a beam-directed CRT driven by an

Incremental Graphics Processor (IGP) interfaced to a PDP 11/45. The computer graphics animation software is based upon standard wireframe drawing techniques and a backline removal algorithm. To produce the simulated satellite motion, the Equations (5) were solved together with damper and kinematic equations, and the computer graphics software calculated the vectors for the CRT as the computer operated at about one frame per second. The system could be interrupted and rerun with parameter changes as desired, by keyboard entry. Representative frames are shown in Figure 10. The viewer is situated on the OZ axis in Figure 10. The system has the capability to provide a view from any location and is thus able to simulate a view of the satellite in geostationary orbit as seen from a given point on earth. A 16 mm film of a representative transition has also been prepared.

To create the display, the f's used in Equations (5) corresponded to a viscous damper about the satellite's roll axis. Although the model did not simulate damping due to the array, fuel slosh, and nutation dampers of Hermes precisely, it enabled a valid demonstration of the qualitative characteristics of the motion. The animation confirmed the characteristics of the transition as described in the previous text. The animation enabled a viewer to develop a conceptual feeling for the transition very quickly, and to identify the important satellite surfaces and attitude motion periods which are relevant to the GEODSS observations.

3.6 THEORY OF LONG TERM BEHAVIOUR OF THE FLAT SPIN RATE

There is no reliable theoretical model available to enable prediction of the long-term behaviour of Hermes' angular momentum vector and flat spin rate, due to absence of flight experience with the particular configuration and orbit. Spin rate changes can be expected due to the solar radiation and earth's magnetic and gravitational fields as is noted in, for example, Reference 5. Based on the previous flight data, the external torques on Hermes are known to be small and hence changes are forecast to occur slowly.

4. CORRELATION OF OBSERVATIONS AND ANALYTICALLY-DERIVED RESULTS

As mentioned earlier the GEODSS ETS observes satellites by detecting and measuring the sunlight reflected from the satellite surfaces. The geometric properties of the satellite reflections are well known (for example Reference 6). The reflected light is described as either a diffuse reflection, having no strongly directional behaviour, or as a specular reflection, which is strongly directional and depends on the surface shape. Specular reflections are usually much brighter than diffuse reflections. The specular reflection of the sun from a flat surface is a beam with a spreading angle of about a half a degree. Such a reflection would seldom be observed from a particular point on the earth's surface. If the flat surface were not smooth, the beam would broaden and decrease in intensity. Specular reflections from the many flat surfaces of the Hermes satellite account for the peaks seen in the satellite brightness noted in Table 1 and Figures 3-4. No attempt has been made to sort out the source of each specular reflection.

Consideration of the observations column of Table 1 and Figures 3-4 in conjunction with the theory and simulation of the previous section leads to the conclusion that two different types of pattern are present.

(a) The observations of Days 331-338 of 1979 have complicated irregular brightness patterns. In the strip chart of Day 335 for example (Figure 3), reflections of several seconds of width and brightness up to ninth magnitude recur at least every 900 seconds and sometimes more often. Also, there are spikes of about 11th magnitude with a period in the range 30 to 150 seconds; the period lengthened as time progressed. This span of observations can be associated with the transition from 3-axis stabilization to flat-spin, as will be described in detail in the next section.

(b) The second distinct type of observation occurs in the data from Day 346, 1979 to Day 52, 1980. Each day shows similar, very regular brightness patterns. Figure 4 is a strip chart of a sample taken from Day 350, 1979. The large but variable (from 13 to 10th magnitude) reflections which were seen irregularly on Days 335-337 are now stable with a period of 292 seconds or greater, with lengthening of the period each day. One set of reflections is noted to have a characteristic double peak. Also, there is an interspersed sequence of broader peaks of variable magnitude. This span of observations can be associated with a flat spin.

4.1 DETAILED CORRELATION FOR THE TRANSITION TO FLAT SPIN

There are two different sets of surfaces on Hermes from the standpoint of visual observation. The sets were identified by studying the computer generated animation of the motion, and the sets can be illustrated by referring to Figure 5. Bear in mind that for the characteristic motion, β is essentially constant for long stretches of time, ψ rotates through 360° slowly with period P_ψ, and the period of rotation P_ω about 02 is short.

(a) The first set consists of the front and back of the array, and the front, back, east, and west sides of the central body. The projection to the viewer of these surfaces is periodic with period P_ω.

(b) The second set consists of the north and south panels and the boom of the solar array. The projection to the viewer of these surfaces does not depend on ϕ or P_ω, but is periodic with period P_ψ.

Equation (14) yields the calculated value of P_ψ of 298 seconds, and it is invariant with β. This period correlates with the observations of Table 1 if the 900 second period is, in fact, three consecutive 300 second periods.

A detailed correlation between the observations of Table 1 and P_ω is given in Table 4. It is hypothesized that the short periods in the observation are created by reflection from the front and back faces of the solar array alternately. The hypothesis leads to a credible history of β, as is shown in Figure 11. Table 4 and Figure 11 are in very good agreement quantitatively with the conclusions drawn from the phase planes of Figures 8-9.

TABLE 4

Measured Periods $T\omega$ and Corresponding Calculated β

Day No.	Short Period in Data	Hypothesis for $T\omega$ (sec)	β Corresponding to $T\omega$ (deg)
329	—	26.4	20
335	24	48	60
336	30-32	61	66
337	40	80	72
338	100-150	250	84
339	spacecraft is rocking	—	87.2
341	as per 339	—	87.2
346	none	Flat Spin	90

4.2 FLAT SPIN AND DESPIN

The reflections observed between Days 346, 1979 and 52, 1980 are attributable to a flat spin configuration. The silver plated array tensioning booms are effectively a specularily-reflecting cylinder. Specular reflections from a cylinder form a cone with a half angle equal to the angle between the cylinder axis pointing away from the sun, and the sun to satellite vector. For the flat spin configuration, where the Hermes satellite spins about an axis perpendicular to the cylinder's axis, the probability of the associated specular reflection being observed at the ETS is high. While other orientations may be possible, a spin axis for Hermes lying in the earth's equatorial plane, perpendicular to the line of sight to the satellite, with the solar panels tilted with respect to the plane of rotation, agrees well with the observed signature (Figure 4). In other words, Hermes appears as a pinwheel on edge when viewed from the ETS.

The rate of flat spin vs time which is derived from the observations is presented in Figure 12. The satellite is noted to despin. The value of the torque required to induce this despin is about 3 micro ft-lb. The cause of this despin is believed to be solar pressure. The two solar sails are believed to be rotated relative to each other to form a propellor. A relative rotational displacement of 2.5° would cause a propellor torque of 3 micro ft-lb.

4.3 THE DOUBLE PEAK AND ARRAY DEFORMATION

The double peak reflection of Figure 4 is believed to be from the silver-plated booms of the solar array. Two peaks are present because there are two booms separated by the central body, and the booms are not quite in line with each other due to bending stresses or misalignment. The timing of the peaks indicates that the relative misalignment angle is about 3.5°. This number is in agreement with the determinations of the dihedral angle made through solar torque observations (Reference 9). The broader peak in Figure 4 is believed to be a reflection from the front side of one of the solar panels or some other more diffuse surface.

5. CONCLUSIONS

Reflections of the sun from the Hermes satellite in synchronous orbit are readily detected by GEODSS. With the dynamic states present after loss of stabilization, the reflections from several of the surfaces typically range from 13th to 11th magnitude and brighter.

The GEODSS optical observations together with a relatively simple dynamics analysis have been sufficient to enable the complex dynamic motion of Hermes to be resolved without ambiguity and monitored. A computer-generated animation of the satellite is noted to have been particularly useful in visualizing the process.

The Hermes satellite made the transition to flat spin from an unstable minimum moment-of-inertia spin state in about 15 days. From this experience, it is concluded that Hermes and spacecraft with similar structural layouts fuel tanks, etc., will remain near the 3-axis oriented state for no more than a day or two in the event of momentum wheel rundown.

The GEODSS data shows that the solar sails are deflected or misaligned in bending relative to each other by about 3.5°. The measurement agrees with other flight data obtained earlier in the mission.

After attainment of flat spin, the satellite was observed to despin to zero rate in about 70 days. The cause of the despin is believed to be a propellor torque associated with relative rotation of about 2.5° between the individual sails.

6. REFERENCES

1. H.R. Raine and J.S. Matsushita, *Hermes Satellite (CTS): Performance and Operations Summary*, AIAA 8th Communications Satellite Systems Conference, April 1980, AIAA Paper No. 80-578.

2. R. Weber, *The Passive, Ground-Based, Electro-Optical Detection of Synchronous Satellites*, TN-1978-27, ESD-TR-78-213, MIT Lincoln Laboratory, Lexington, Mass., 19 June 1978.

3. W.T. Thomson and G.S. Reiter, *Attitude Drift of Space Vehicles*, The Journal of the Astronautical Sciences, Vol. VII, No. 1, Summer 1960.

4. F.R. Vigneron, *Motion of a Freely Spinning Gyrostat Satellite with Energy Dissipation*, Astronautica Acta, Vol. 16, 1971, pp. 373-380.

5. F.R. Vigneron, *Dynamics of Alouette and ISIS Satellites*, Astronautica Acta, Vol. 18, 1973, pp. 201-213.

6. G.A. McCue, J.G. Williams, J.M. Morford, *Optical Characteristics of Artificial Satellites*, Planetary Space Science, Vol. 19, p. 851, 1971.

7. T.D. Harrison, G.B. Lang, V. Gore, F. Vigneron and E. Quittner, *In-Orbit Characteristics of the Communications Technology Satellite Deployable Solar Array*, Eleventh Intersociety Energy Conversion Engineering Conference, Tahoe, 1976.

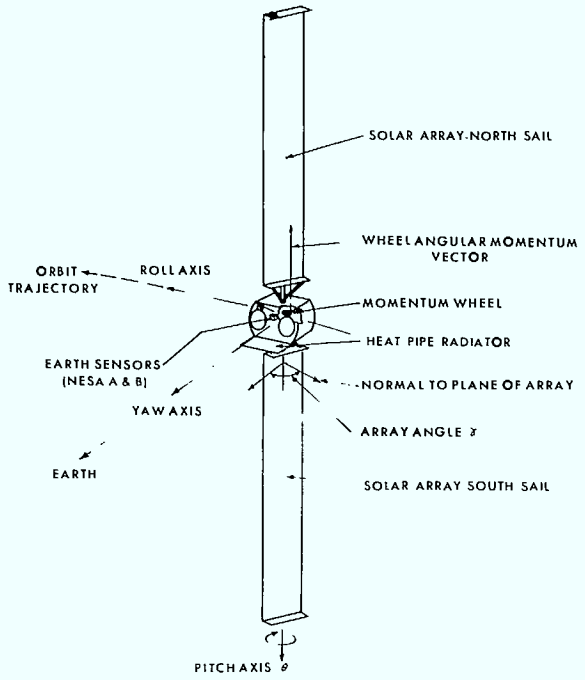

Figure 1. Hermes On-Orbit Configuration with the Array Fully Deployed

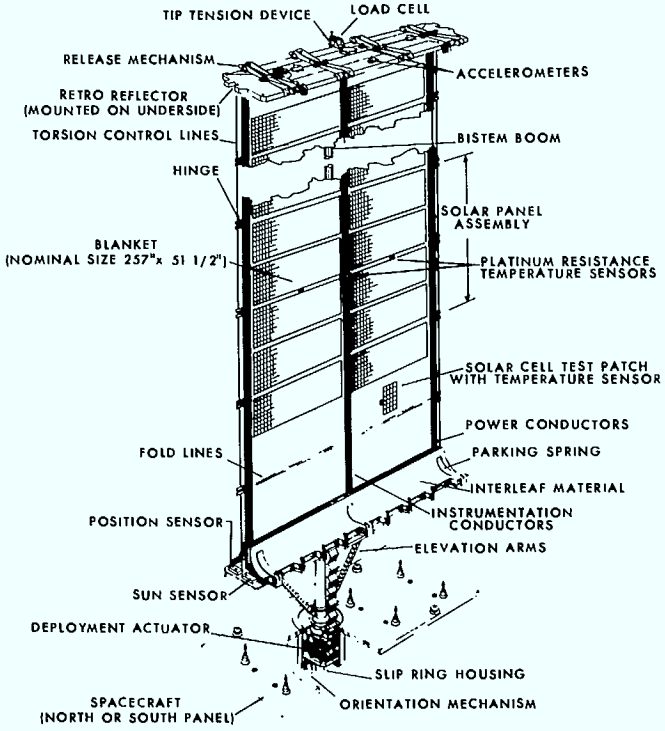

Figure 2. Schematic of One Solar Sail, showing the Silver-Plated 1 3/8" BISTEM Boom and Semi-Transparent Kapton Substrate

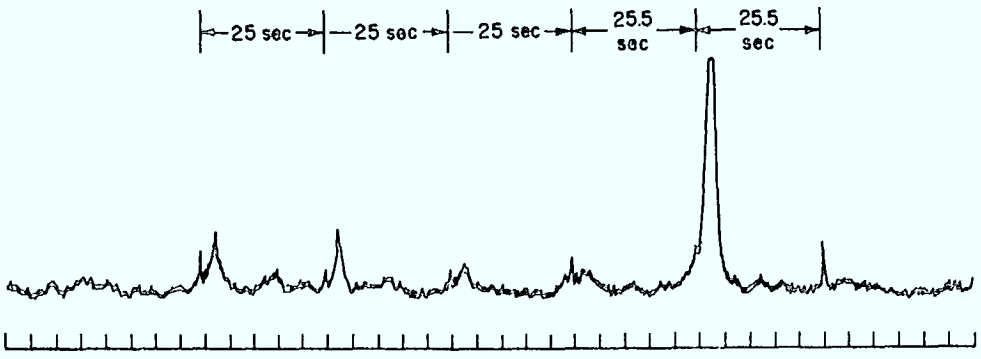

Figure 3. Brightness variation on Day 335. Time increases toward the left, and increased brightness is toward the top of the figure. The time scale is five seconds per division. The series of sharp spikes appear to represent a relatively fast rotation around one satellite axis. The spikes are approximately 11^m visual magnitudes.

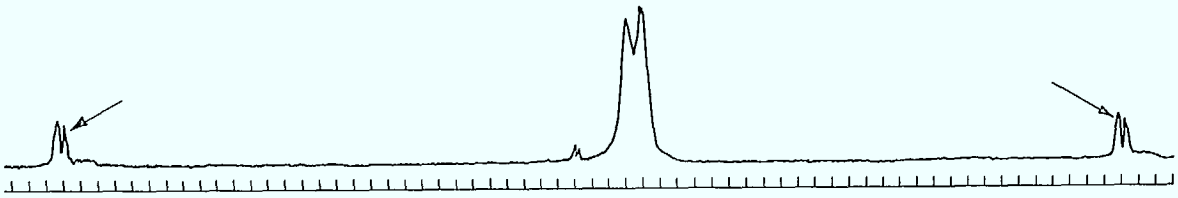

(a) at 500 GMT

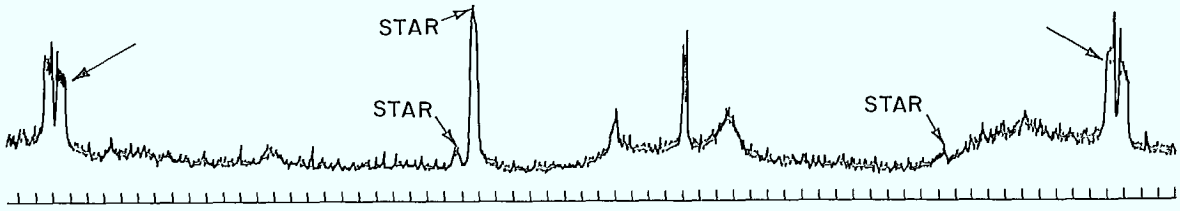

(b) at 0800 GMT

Figure 4. Brightness Variation of Hermes on Day 350. For both curves time increases to the left, and the time scale is 5 seconds per division. Increased brightness is to the top of the figure. The strip chart recorder gain was adjusted to keep the high intensity peaks on the chart. The separation of the double peaks (indicated by arrows) measures the rotation period of the satellite. The double peaks were approximately constant in intensity from Day 339 of 1979 to Day 52 of 1980. Note that the signature structure near the center changes in relative position as well as intensity.

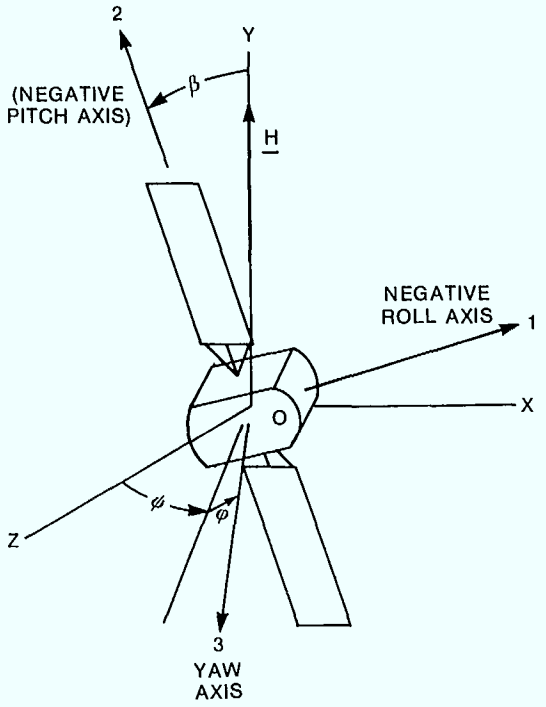

Figure 5. Satellite and coordinates. The Euler angles ψ, β, and ϕ are a (2, 3, 2) rotation sequence.

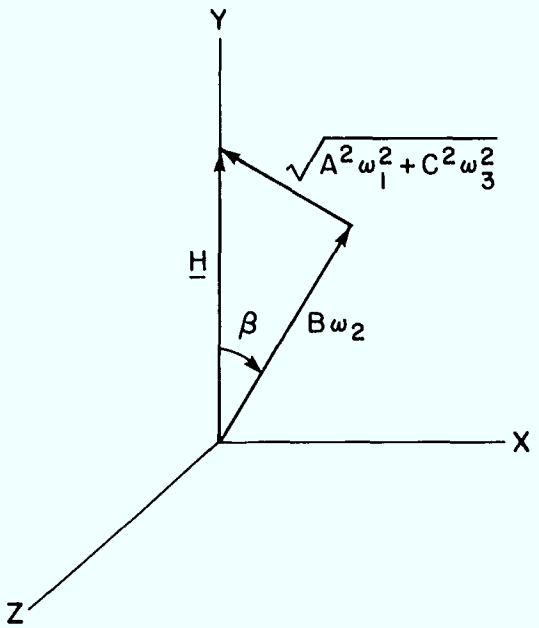

Figure 6. H and its Components

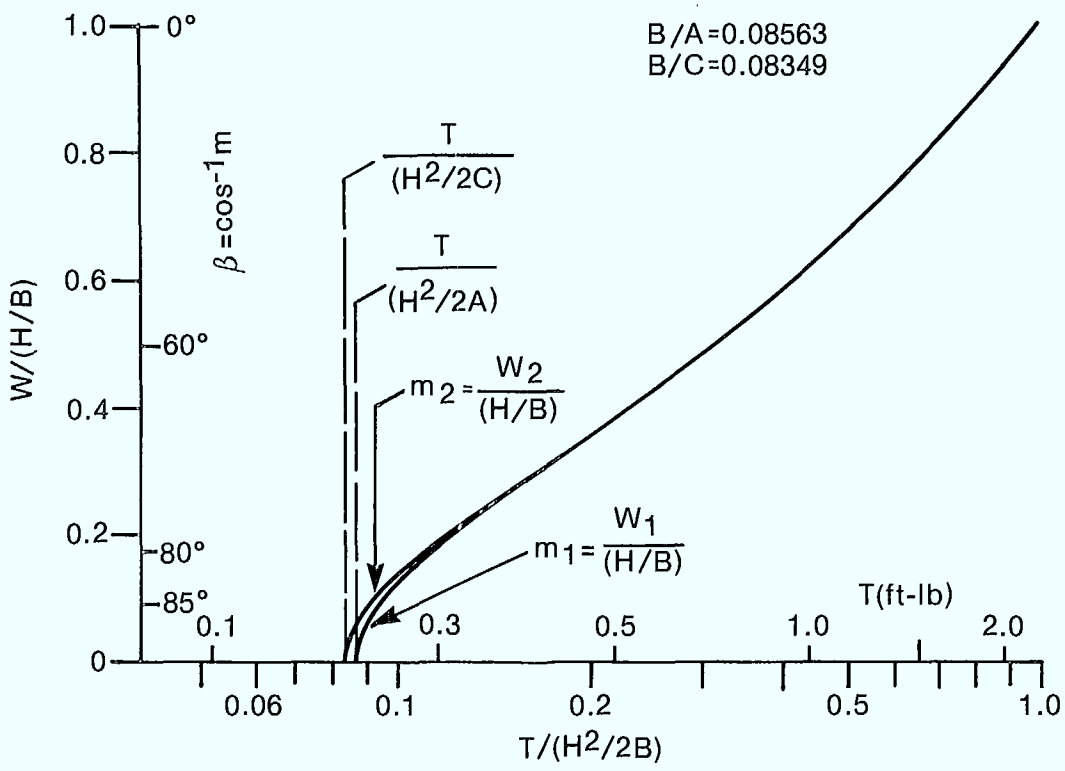

Figure 7. W_1, W_2 and direction cosines m_1, m_2 vs. T. Presented in dimensionless form. For Hermes, H/B = 0.253 rad/sec and $H^2/2B$ = 2.291 lb-ft., A =835.0 slug-ft.^{2}, B = 71.5 slug-ft^2, C = 856.4 slug-ft^2.

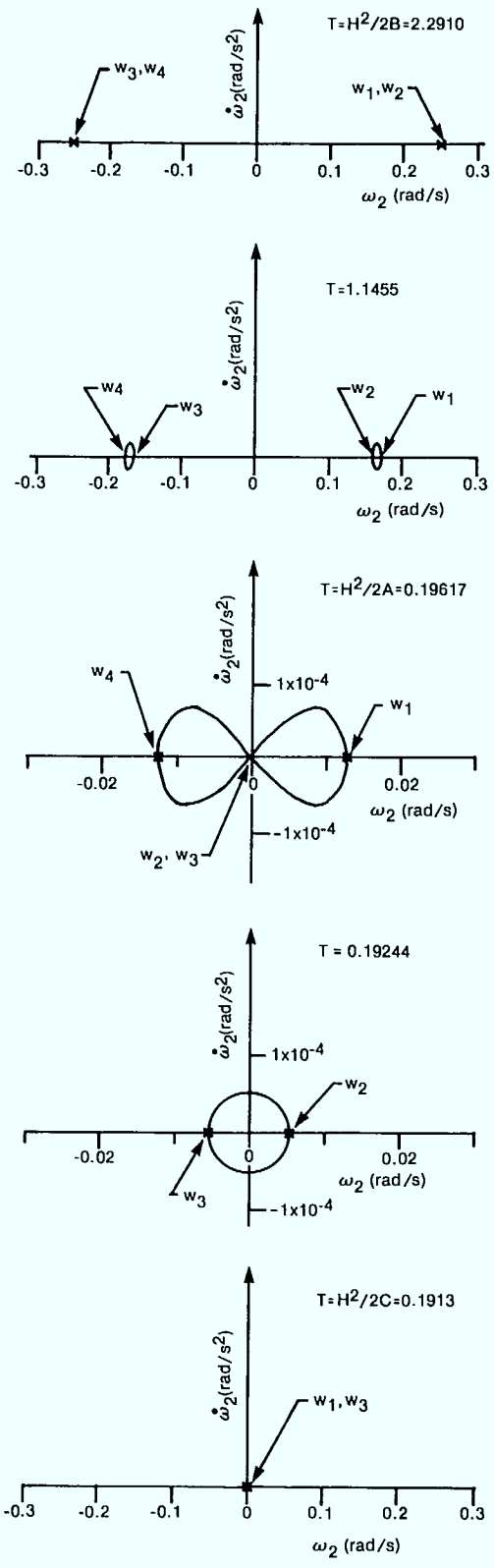

Figure 8. Phase Planes for ω_2

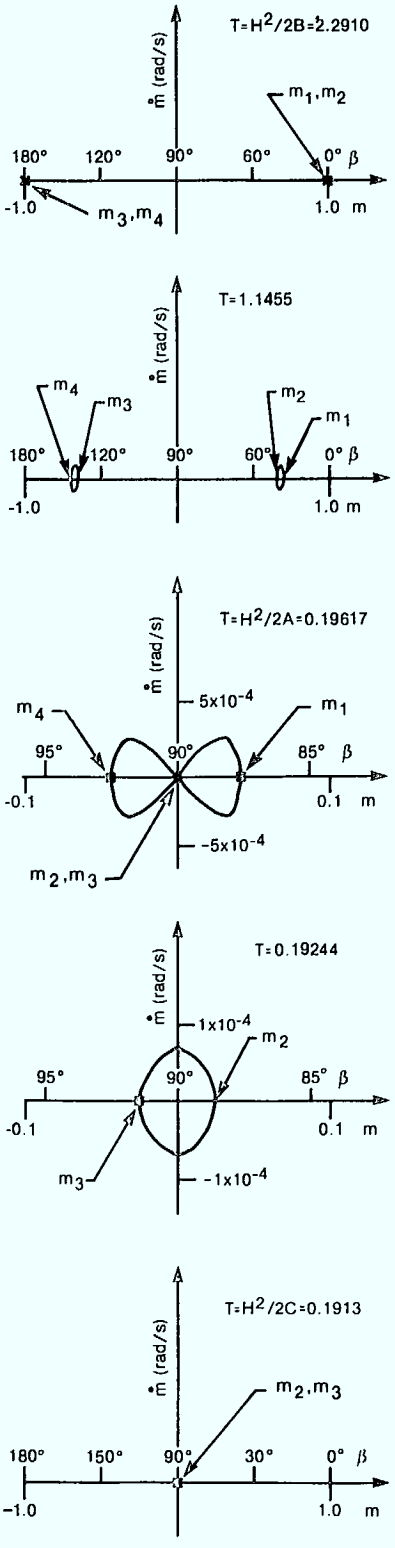

Figure 9. Phase Planes for $m = cos_{\beta}$

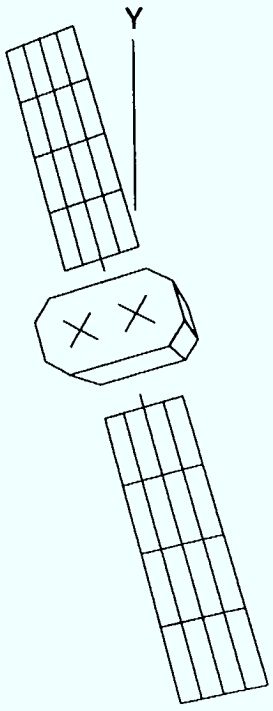

(a) About Day 330, $\beta = 20^{\circ}$

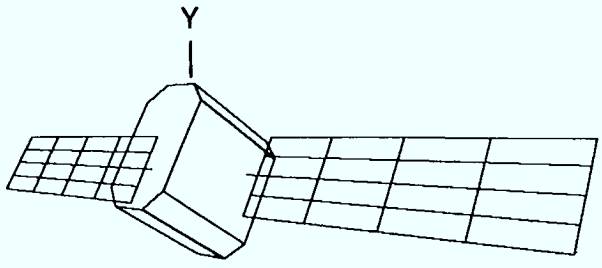

(b) About Day 339, $\beta = 80\text{-}88^{\circ}$ and Satellite is Rocking about Pitch

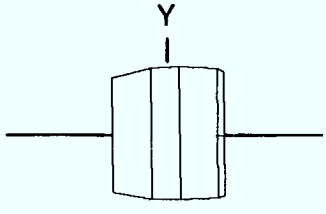

(c) About Day 346, $\beta = 90^{\circ}$, Spin about Maximum Moment of Inertia Axis

Figure 10. Representative Frames of the Computer Generated Animation

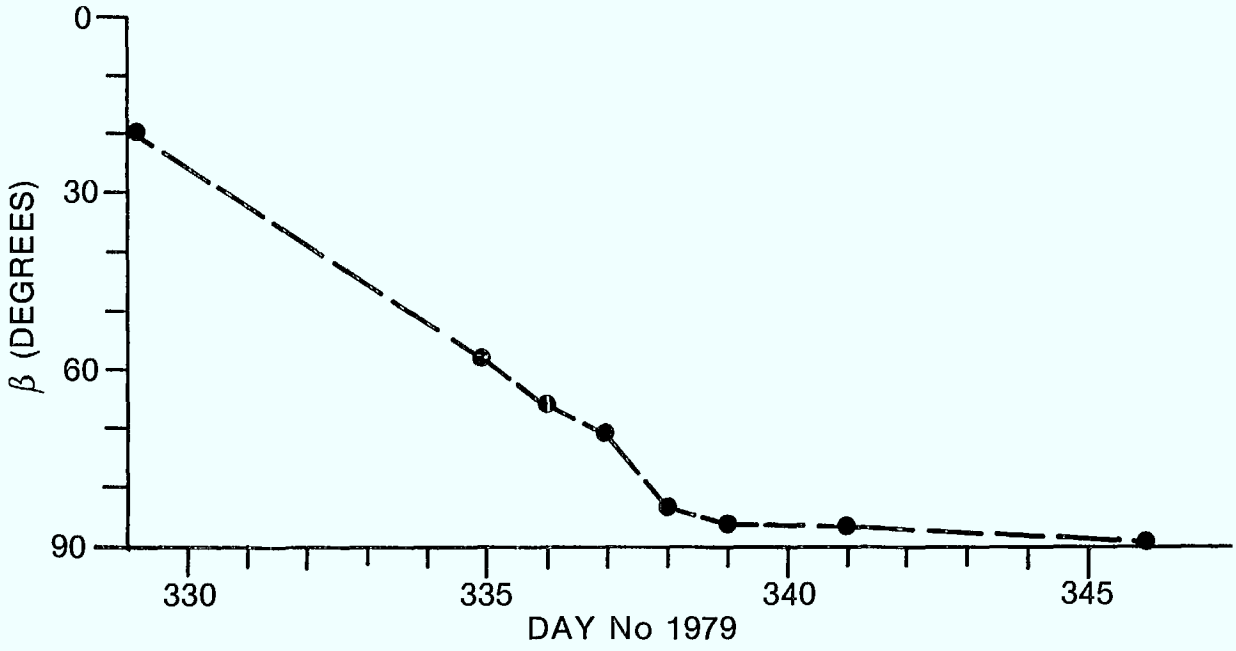

Figure 11. β Vs. Day Number, as Calculated from Measurements of P_ω and Equation (13)

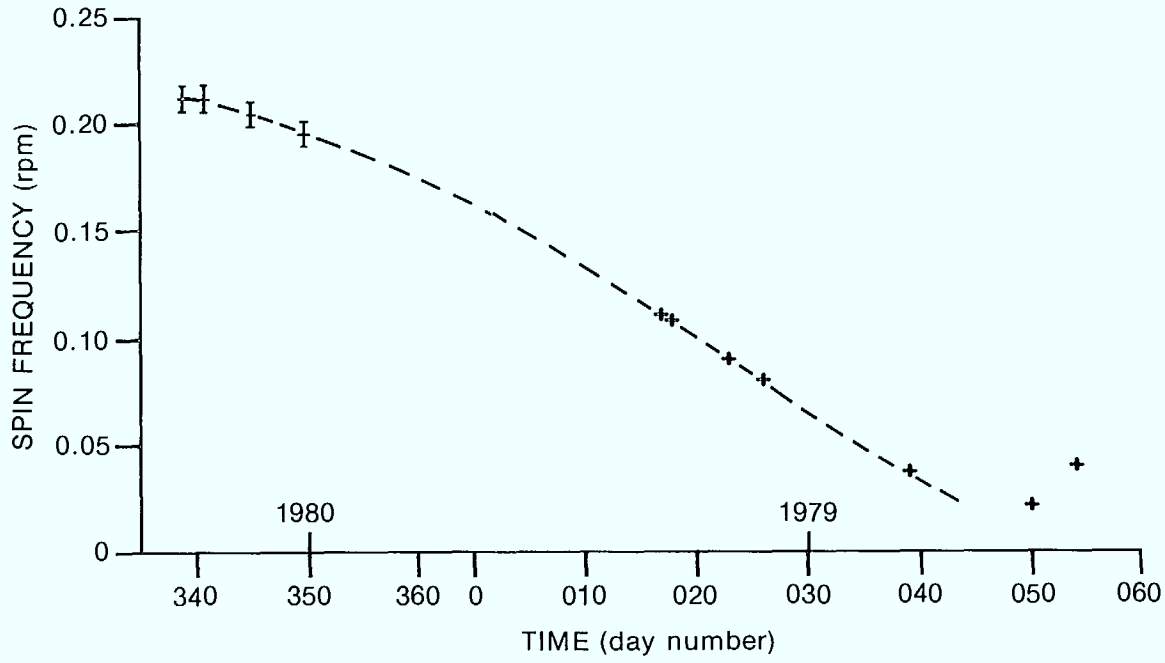

Figure 12. A plot of the "flat spin" frequency as a function of time. The spin frequency is measured by the inverse of the time between successive appearances of the doublet peaks shown in Figure 4.

CRC DOCUMENT CONTROL DATA

1. **ORIGINATOR:** Department of Communications/Communications Research Centre

2. **DOCUMENT NO:** CRC Report No. 1354

3. **DOCUMENT DATE:** February 1982

4. **DOCUMENT TITLE:** The Attitude Dynamics of Hermes after Termination of Three-Axis Stabilization

5. **AUTHOR(s):** F.R. Vigneron and W.E. Krag

6. **KEYWORDS:** (1) Attitude
(2) Dynamics
(3) Hermes

7. **SUBJECT CATEGORY (FIELD & GROUP: COSATI)**

22 Space Technology

22 02 Spacecraft

8. **ABSTRACT:** In late 1979, Hermes, an experimental geostationary communications satellite, experienced an earth sensor malfunction which resulted in its loss of control and subsequent transition from 3-axis stabilization to spin about its maximum-moment-of-inertia axis. During and after the transition, the sun's reflections from the satellite were detected and monitored at the experimental test site (ETS) for the Ground Based Electro Optical Deep Space Surveillance System (GEODSS) in New Mexico. In this report, the satellite's attitude dynamics are deduced by correlating the GEODSS ETS observations with dynamics analysis and simulation. The transition to spin took about 15 days. Thereafter, the rate of spin decayed to zero in about 70 days due to solar pressure. The GEODSS ETS observations also provide data on the relative misalignment and bending of the two solar sails of the satellite.

9. **CITATION:**

Government of Canada Gouvernement du Canada